Enhancement of nonlocality in phase space

Stefano Olivares* and Matteo G. A. Paris†
Dipartimento di Fisica dell'Università degli Studi di Milano, Milano, Italy
(Received 4 June 2004; published 29 September 2004)

We show that inconclusive photon subtraction (IPS) on a twin beam produces non-Gaussian states that violate Bell's inequality in the phase space. The violation is larger than for the twin beam itself irrespective of the IPS quantum efficiency. The explicit expression for the IPS map is given both for the density matrix and the Wigner function representations.

DOI: 10.1103/PhysRevA.70.032112 PACS number(s): 03.65.Ud, 03.67.Mn

I. INTRODUCTION

The twin-beam (TWB) state of two modes of radiation can be expressed in the photon number basis as

$$|\Lambda\rangle\rangle_{ab} = \sqrt{1-\lambda^2}\sum_{n=0}^{\infty} \lambda^n |n,n\rangle_{ab}, \tag{1}$$

where $\lambda = \tanh(r)$, r being the TWB squeezing parameter. The TWB state is described by a Gaussian Wigner function

$$W_r(\alpha,\beta) = \frac{4}{\pi^2} \exp\{-2A(|\alpha|^2 + |\beta|^2) + 2B(\alpha\beta + \overline{\alpha}\overline{\beta})\}, \tag{2}$$

with $A \equiv A(r) = \cosh(2r)$ and $B \equiv B(r) = \sinh(2r)$. Since Eq. (2) is positive definite, TWBs are not suitable to test nonlocality through homodyne detection. Indeed, the Wigner function itself provides an explicit hidden variable model for homodyne measurements [1,2]. On the other hand, it has been shown [2] that a TWB state exhibits a nonlocal character for parity measurements. This is known as nonlocality in the phase space since Bell inequalities can be written in terms of the Wigner function, which in turn describes correlations for the joint measurement of displaced parity operators. Overall, the positivity or the negativity of the Wigner function has a rather weak relation to the locality or the nonlocality of quantum correlations.

In Ref. [5] we suggested a conditional measurement scheme on TWBs leading to a non-Gaussian entangled mixed state, which improves fidelity in the teleportation of coherent states. This process, called inconclusive photon subtraction (IPS), is based on mixing each mode of the TWB with the vacuum in an unbalanced beam splitter and then performing inconclusive photodetection on both modes, i.e., revealing the reflected beams without discriminating the number of detected photons.

A single-mode version of the IPS, mapping squeezed light onto non-Gaussian states, has been recently realized experimentally [6]. Moreover, IPS has been suggested as a feasible method to modify the TWB state and test nonlocality using homodyne detection [3,4].

In this paper we address IPS as a *de-Gaussification* map for a TWB, give its explicit expression for the density matrix and the Wigner function, and investigate the nonlocality of the resulting state in the phase space.

The paper is structured as follows. In Sec. II we review nonlocality in the phase space, i.e., the Wigner function Bell's inequality based on measuring the displaced parity operator on two modes of radiation. In Sec. III we illustrate the IPS process as a de-Gaussification map and calculate the Wigner function of the IPS state. The nonlocality of the IPS state in the phase space is then analyzed in Sec. IV, whereas in Sec. V we discuss nonlocality using homodyne detection, extending the analysis of Refs. [3] and [4]. Section VI closes the paper with some concluding remarks.

II. NONLOCALITY IN THE PHASE SPACE

The displaced parity operator on two modes is defined as

$$\hat{\Pi}(\alpha,\beta) = D_a(\alpha)(-1)^{a^\dagger a} D_a^\dagger(\alpha) \otimes D_b(\beta)(-1)^{b^\dagger b} D_b^\dagger(\beta), \tag{3}$$

where α, $\beta \in \mathbb{C}$, a, and b are mode operators, and $D_a(\alpha) = \exp\{\alpha a^\dagger - \overline{\alpha} a\}$ and $D_b(\beta)$ are single-mode displacement operators. Parity is a dichotomic variable and thus can be used to establish Bell-like inequalities [7]. Since the two-mode Wigner function $W(\alpha,\beta)$ can be expressed as

$$W(\alpha,\beta) = \frac{4}{\pi^2}\Pi(\alpha,\beta), \tag{4}$$

$\Pi(\alpha,\beta)$ being the expectation value of $\hat{\Pi}(\alpha,\beta)$, the violation of these inequalities is also known as nonlocality in the phase space. The quantity involved in such inequalities can be written as follows:

$$\mathcal{B} = \Pi(\alpha_1,\beta_1) + \Pi(\alpha_2,\beta_1) + \Pi(\alpha_1,\beta_2) - \Pi(\alpha_2,\beta_2), \tag{5}$$

which, for local theories, satisfies the condition $|\mathcal{B}| \leqslant 2$.

Following Ref. [2], one can choose a particular set of displaced parity operators, arriving at the combination

*Electronic address: Stefano.Olivares@mi.infn.it
†Electronic address: Matteo.Paris@fisica.unimi.it

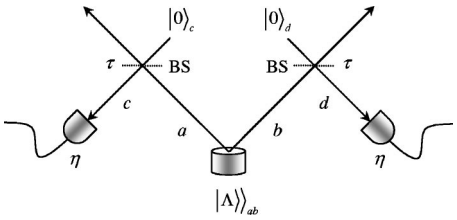

FIG. 1. Scheme of the IPS process.

$$B(J) = \Pi(0,0) + \Pi(\sqrt{J},0) + \Pi(0,-\sqrt{J}) - \Pi(\sqrt{J},-\sqrt{J}), \tag{6}$$

which depends only on the positive parameter J, characterizing the magnitude of the displacement. If we evaluate the quantity (6) in the case of the TWB, we find that it exceeds the upper bound imposed by local theories for a certain region of values (J,r), its maximum being $B \approx 2.19$ [2].

On the other hand, the choice of the parameters leading to Eq. (6) is not the best one, and the violation of the inequality $|\mathcal{B}| \leqslant 2$ can be enhanced using a different parametrization [8]. A better result is achieved for

$$C(J) = \Pi(\sqrt{J},-\sqrt{J}) + \Pi(-3\sqrt{J},-\sqrt{J}) + \Pi(\sqrt{J},3\sqrt{J}) - \Pi(-3\sqrt{J},3\sqrt{J}), \tag{7}$$

which, for the TWB, gives a maximum $C \approx 2.32$, greater than the value 2.19 obtained in Ref. [2]. Notice that, even in the infinite squeezing limit, the violation is never maximal, i.e., $|\mathcal{B}| < 2\sqrt{2}$ [9].

In the following sections we will see that the violation of the inequalities $|B(J)| \leqslant 2$ and $|C(J)| \leqslant 2$ can be enhanced by de-Gaussification of the TWB.

III. THE DE-GAUSSIFICATION PROCESS

The de-Gaussification of a TWB can be achieved by subtracting photons from both modes [5,10,11]. In Ref. [5] we referred to this process as to inconclusive photon subtraction and showed that the resulting state, the IPS state $\varrho_{\rm IPS}$, can be used to enhance the teleportation fidelity of coherent states for a wide range of the experimental parameters.

The IPS scheme is sketched in Fig. 1. The two modes a and b of the TWB are mixed with the vacuum (modes c and d, respectively) at two unbalanced beam splitters (BSs) with equal transmissivity $\tau = \cos^2\phi$; the modes c and d are then revealed by avalanche photodetectors (APDs) with equal efficiency η. APDs can discriminate only the presence of radiation from the vacuum. The positive-operator-valued measure (POVM) $\{\Pi_0(\eta), \Pi_1(\eta)\}$ of each detector is given by

$$\Pi_0(\eta) = \sum_{j=0}^{\infty} (1-\eta)^j |j\rangle\langle j|, \quad \Pi_1(\eta) = \mathbb{I} - \Pi_0(\eta), \tag{8}$$

η being the quantum efficiency. Overall, the conditional measurement on the modes c and d is described by the POVM (we are assuming the same quantum efficiency for both photodetectors)

$$\Pi_{00}(\eta) = \Pi_{0,c}(\eta) \otimes \Pi_{0,d}(\eta), \tag{9}$$

$$\Pi_{01}(\eta) = \Pi_{0,c}(\eta) \otimes \Pi_{1,d}(\eta), \tag{10}$$

$$\Pi_{10}(\eta) = \Pi_{1,c}(\eta) \otimes \Pi_{0,d}(\eta), \tag{11}$$

$$\Pi_{11}(\eta) = \Pi_{1,c}(\eta) \otimes \Pi_{1,d}(\eta). \tag{12}$$

When the two photodetectors jointly click, the conditioned output state of modes a and b is given by

$$\mathcal{E}(R) = \frac{1}{p_{11}(r,\phi,\eta)} \mathrm{Tr}_{cd}[U_{ac}(\phi) \otimes U_{bd}(\phi) R \otimes |0\rangle_{cc}\langle 0| \otimes |0\rangle_{dd}\langle 0| U_{ac}^{\dagger}(\phi) \otimes U_{bd}^{\dagger}(\phi) \mathbb{I}_a \otimes \mathbb{I}_b \otimes \Pi_{11}(\eta)], \tag{13}$$

where $U_{ac}(\phi) = \exp\{-\phi(a^{\dagger}c - ac^{\dagger})\}$ and $U_{bd}(\phi)$ are the evolution operators of the beam splitters and R the density operator of the two-mode state entering the beam splitters (in our case $R = \varrho_{\rm TWB} = |\Lambda\rangle\rangle_{abba}\langle\langle\Lambda|$). The partial trace on modes c and d can be explicitly evaluated, thus arriving at the Kraus decomposition of the IPS map. We have

$$\mathcal{E}(R) = \frac{1}{p_{11}(r,\phi,\eta)} \sum_{p,q=1}^{\infty} m_p(\phi,\eta) M_{pq}(\phi) R M_{pq}^{\dagger}(\phi) m_q(\phi,\eta) \tag{14}$$

with

$$m_p(\phi,\eta) = \frac{\tan^{2p}\phi\,[1-(1-\eta)^p]}{p!} \tag{15}$$

and

$$M_{pq}(\phi) = a^p b^q (\cos\phi)^{a^{\dagger}a + b^{\dagger}b}, \tag{16}$$

and

$$p_{11}(r,\phi,\eta) = \mathrm{Tr}_{ab}[\mathcal{E}(R)] \tag{17}$$

is the probability of a click in both detectors.

Now, in order to investigate the nonlocality of the state $\varrho_{\rm IPS} = \mathcal{E}(\varrho_{\rm TWB})$ in the phase space, we explicitly calculate its Wigner function, which, as one may expect, is no longer Gaussian and positive definite.

The state entering the two beam splitters is described by the Wigner function

$$W_r^{(\rm in)}(\alpha,\beta,\zeta,\xi) = W_r(\alpha,\beta)\frac{4}{\pi^2}\exp\{-2|\zeta|^2 - 2|\xi|^2\}, \tag{18}$$

where the second factor on the right hand side represents the two vacuum states of modes c and d. The action of the beam splitters on $W_r^{(\rm in)}$ can be summarized by the following change of variables:

$$\alpha \to \alpha\cos\phi + \zeta\sin\phi, \quad \zeta \to \zeta\cos\phi - \alpha\sin\phi, \tag{19}$$

$$\beta \to \beta\cos\phi + \xi\sin\phi, \quad \xi \to \xi\cos\phi - \beta\sin\phi, \tag{20}$$

and the output state, after the beam splitters, is then given by

$$W^{(\mathrm{out})}_{r,\phi}(\alpha,\beta,\zeta,\xi) = \frac{4}{\pi^2} W_{r,\phi}(\alpha,\beta)\exp\{-a|\xi|^2 + w\xi + \overline{w}\overline{\xi}\} \times \exp\{-a|\zeta|^2 + (v + 2B\xi\sin^2\phi)\zeta + (\overline{v} + 2B\overline{\xi}\sin^2\phi)\overline{\zeta}\}, \quad (21)$$

where

$$W_{r,\phi}(\alpha,\beta) = \frac{4}{\pi^2}\exp\{-b(|\alpha|^2 + |\beta|^2) + 2B\cos^2\phi\,(\alpha\beta + \overline{\alpha}\overline{\beta})\} \quad (22)$$

and

$$a \equiv a(r,\phi) = 2(A\sin^2\phi + \cos^2\phi), \quad (23)$$

$$b \equiv b(r,\phi) = 2(A\cos^2\phi + \sin^2\phi), \quad (24)$$

$$v \equiv v(r,\phi) = 2\cos\phi\sin\phi\,[(1-A)\overline{\alpha} + B\beta], \quad (25)$$

$$w \equiv w(r,\phi) = 2\cos\phi\sin\phi\,[(1-A)\overline{\beta} + B\alpha]. \quad (26)$$

At this stage conditional on/off detection is performed on modes c and d (see Fig. 1). We are interested in the situation when both the detectors click. The Wigner function of the double click element $\Pi_{11}(\eta)$ of the POVM [see Eq. (12)] is given by [5,12]

$$W_\eta(\zeta,\xi) \equiv W[\Pi_{11}(\eta)](\zeta,\xi) = \frac{1}{\pi^2}\{1 - Q_\eta(\zeta) - Q_\eta(\xi) + Q_\eta(\zeta)Q_\eta(\xi)\}, \quad (27)$$

with

$$Q_\eta(z) = \frac{2}{2-\eta}\exp\left\{-\frac{2\eta}{2-\eta}|z|^2\right\}. \quad (28)$$

Using Eq. (13) and the phase-space expression of the trace (for each mode)

$$\mathrm{Tr}[O_1O_2] = \pi\int_{\mathbb{C}} d^2z\, W[O_1](z)W[O_2](z), \quad (29)$$

O_1 and O_2 being two operators and $W[O_1](z)$ and $W[O_2](z)$ their Wigner functions, respectively, the Wigner function of the output state, conditioned to the double-click event, is then given by

$$W_{r,\phi,\eta}(\alpha,\beta) = \frac{f_{r,\phi,\eta}(\alpha,\beta)}{p_{11}(r,\phi,\eta)}, \quad (30)$$

where

$$f_{r,\phi,\eta}(\alpha,\beta) = \pi^2\int_{\mathbb{C}^2} d^2\zeta d^2\xi \frac{4}{\pi^2} W_{r,\phi}(\alpha,\beta)\sum_{j=1}^{4}\frac{C_j(\eta)}{\pi^2} \times G^{(j)}_{r,\phi,\eta}(\alpha,\beta,\zeta,\xi), \quad (31)$$

and $p_{11}(r,\phi,\eta)$ is the double-click probability (17), which can be written as a function of $f_{r,\phi,\eta}(\alpha,\beta)$ as follows:

TABLE I. Expressions of C_j, x_j, and y_j appearing in Eq. (33).

j	$x_j(r,\phi,\eta)$	$y_j(r,\phi,\eta)$	$C_j(\eta)$
1	a	a	1
2	$a + \frac{2}{2-\eta}$	a	$-\frac{2}{2-\eta}$
3	a	$a + \frac{2}{2-\eta}$	$-\frac{2}{2-\eta}$
4	$a + \frac{2}{2-\eta}$	$a + \frac{2}{2-\eta}$	$\left(\frac{2}{2-\eta}\right)^2$

$$p_{11}(r,\phi,\eta) = \pi^2\int_{\mathbb{C}^2} d^2\alpha d^2\beta f_{r,\phi,\eta}(\alpha,\beta). \quad (32)$$

The quantity $G^{(j)}_{r,\phi,\eta}(\alpha,\beta,\zeta,\xi)$ appearing in Eq. (31) is

$$G^{(j)}_{r,\phi,\eta}(\alpha,\beta,\zeta,\xi) = \exp\{-x_j|\zeta|^2 + (v + 2B\xi\sin^2\phi)\zeta + (\overline{v} + 2B\overline{\xi}\sin^2\phi)\overline{\zeta}\} \times \exp\{-y_j|\xi|^2 + w\xi + \overline{w}\overline{\xi}\}, \quad (33)$$

and the expressions of $C_j(\eta)$, $x_j \equiv x_j(r,\phi,\eta)$, and $y_j \equiv y_j(r,\phi,\eta)$ are given in Table I.

The mixing with the vacuum in a beam splitter with transmissivity τ followed by on/off detection with quantum efficiency η is equivalent to mixing with an effective transmissivity [5]

$$\tau_{\mathrm{eff}} \equiv \tau_{\mathrm{eff}}(\phi,\eta) = 1 - \eta(1-\tau) \quad (34)$$

followed by an ideal (i.e., efficiency equal to 1) on/off detection. Therefore, the state (30) can be studied for $\eta = 1$ and replacing τ with τ_{eff}. Thanks to this substitution, after the integrations we have

$$f_{r,\phi,\eta}(\alpha,\beta) = \frac{1}{\pi^2}\sum_{j=1}^{4}\frac{16C_j(\eta)}{x_jy_j - 4B^2(1-\tau_{\mathrm{eff}})^2}\exp\{-(b-f_j)|\alpha|^2 - (b-g_j)|\beta|^2 + (2B\tau_{\mathrm{eff}} + h_j)(\alpha\beta + \overline{\alpha}\overline{\beta})\} \quad (35)$$

and

$$p_{11}(r,\phi,\eta) = \sum_{j=1}^{4}\frac{16[x_jy_j - 4B^2(1-\tau_{\mathrm{eff}})^2]^{-1}C_j(\eta)}{(b-f_j)(b-g_j) - (2Bh_j\tau_{\mathrm{eff}})^2}, \quad (36)$$

where we defined

$$f_j \equiv f_j(r,\phi,\eta) = N_j[x_j(1-A)^2 + 4B^2(1-A)(1-\tau_{\mathrm{eff}}) + y_jB^2], \quad (37)$$

$$g_j \equiv g_j(r,\phi,\eta) = N_j[x_jB^2 + 4B^2(1-A)(1-\tau_{\mathrm{eff}}) + y_j(1-A)^2], \quad (38)$$

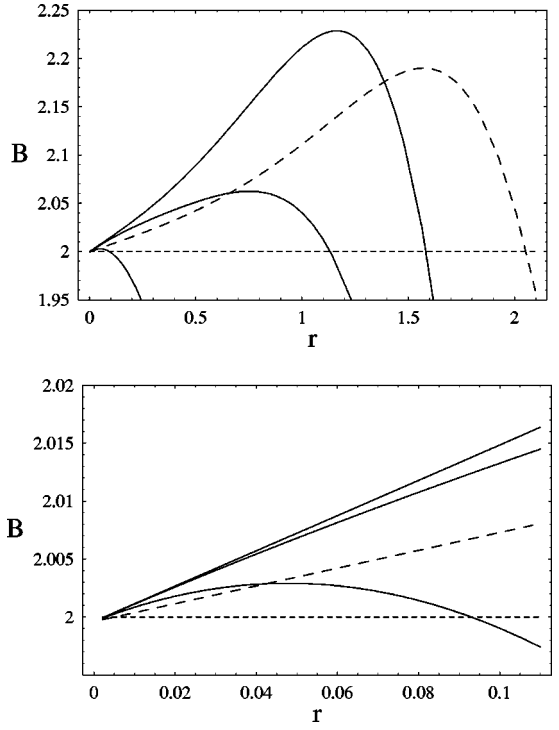

FIG. 2. Plot of $B(J)$ given in Eq. (6) for $J=10^{-2}$. The dashed line is $B_r^{(\mathrm{TWB})}(J)$, while the solid lines are $B_{r,\phi,\eta}^{(\mathrm{IPS})}(J)$ for different values of τ_{eff} (see the text): from top to bottom $\tau_{\mathrm{eff}}=0.999$, 0.99, and 0.9. When $\tau_{\mathrm{eff}}=0.999$, the maximum of $B_{r,\phi,\eta}^{(\mathrm{IPS})}(J)$ is 2.23. The lower plot is a magnification of the region $0\leqslant r\leqslant 0.11$ of the upper one. Notice that for small r there is always a region where $B_r^{(\mathrm{TWB})}(J)<B_{r,\phi,\eta}^{(\mathrm{IPS})}(J)$.

$$h_j \equiv h_j(r,\phi,\eta) = N_j\{(x_j+y_j)B(1-A)+4B[B^2+(1-A)^2](1-\tau_{\mathrm{eff}})\}, \tag{39}$$

$$N_j \equiv N_j(r,\phi,\eta) = \frac{4\tau_{\mathrm{eff}}(1-\tau_{\mathrm{eff}})}{x_j y_j - 4B^2(1-\tau_{\mathrm{eff}})^2}. \tag{40}$$

In this way, the Wigner function of the IPS state can be rewritten as

$$W_{r,\phi,\eta}(\alpha,\beta) = W_{r,\phi}(\alpha,\beta)\sum_{j=1}^{4}\frac{4C_j(\eta)K_{r,\phi,\eta}^{(j)}(\alpha,\beta)}{p_{11}(r,\phi,\eta)[x_j y_j - 4B^2(1-\tau_{\mathrm{eff}})^2]}, \tag{41}$$

where we introduced

$$K_{r,\phi,\eta}^{(j)}(\alpha,\beta) = \exp\{f_j|\alpha|^2 + g_j|\beta|^2 + h_j(\alpha\beta+\overline{\alpha}\overline{\beta})\}. \tag{42}$$

The state given in Eq. (41) is no longer a Gaussian state.

IV. NONLOCALITY OF THE IPS STATE

In this section we investigate the nonlocality of the state (41) in phase space using the quantity $\mathcal{B}$ given in Eq. (5), referring to both the parametrizations $B(J)$ [see Eq. (6)] and $C(J)$ [see Eq. (7)].

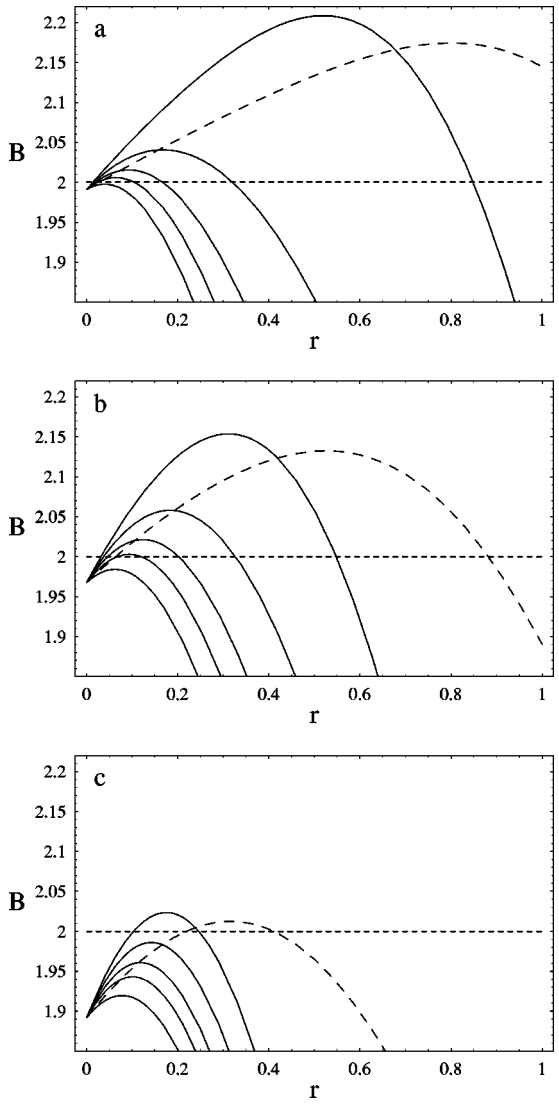

FIG. 3. Plots of $B(J)$ given in Eq. (6) as a function of the squeezing parameter r for different values of J: (a) $J=5\times10^{-2}$, (b) $J=10^{-1}$, and (c) $J=2\times10^{-1}$. In all the plots the dashed line is $B_r^{(\mathrm{TWB})}(J)$, while the solid lines are $B_{r,\phi,\eta}^{(\mathrm{IPS})}(J)$ for different values of τ_{eff} (see the text): from top to bottom $\tau_{\mathrm{eff}}=0.999$, 0.9, 0.8, 0.7, and 0.5. Notice that there is always a region for small r where $B_r^{(\mathrm{TWB})}(J)<B_{r,\phi,\eta}^{(\mathrm{IPS})}(J)$. When $\tau_{\mathrm{eff}}=0.999$ the maximum of $B_{r,\phi,\eta}^{(\mathrm{IPS})}(J)$ is always greater than that of $B_r^{(\mathrm{TWB})}(J)$.

As for a TWB, the violation of the Bell's inequality is observed for small r [2]. From now on, we will refer to $B(J)$ as $B_r^{(\mathrm{TWB})}(J)$ when it is evaluated for a TWB (2), and as $B_{r,\phi,\eta}^{(\mathrm{IPS})}(J)$ when we consider the IPS state (41). We plot $B_r^{(\mathrm{TWB})}(J)$ and $B_{r,\phi,\eta}^{(\mathrm{IPS})}(J)$ in Figs. 2 and 3 for different values of the effective transmissivity τ_{eff} and of the parameter J: for not too big values of the squeezing parameter r, one has that $2<B_{r,\phi,\eta}^{(\mathrm{TWB})}(J)<B_{r,\phi,\eta}^{(\mathrm{IPS})}(J)$. Moreover, when τ_{eff} approaches unity, i.e., when at most one photon is subtracted from each mode, the maximum of $B_{r,\phi,\eta}^{(\mathrm{IPS})}$ is always greater than the one obtained using a TWB. A numerical analysis shows that in the limit $\tau_{\mathrm{eff}}\to1$ the maximum is 2.27, which is greater than the value 2.19 obtained for a TWB [2]. The

limit $\tau_{\rm eff}\to 1$ corresponds to the case of one single photon subtracted from each mode [10,11]. Notice that increasing J reduces the interval of the values of r for which one has the violation. For large r the best result is thus obtained with the TWB since, as the energy grows, more photons are subtracted from the initial state [5]. Since the relevant parameter for violation of Bell inequalities is $\tau_{\rm eff}$, we have, from Eq. (34), that the IPS state is nonlocal also for low quantum efficiency of the IPS detector.

The same conclusions hold when we consider the parametrization of Eq. (7). In Fig. 4 we plot $C_r^{(\rm TWB)}(J)$ and $C_{r,\phi,\eta}^{(\rm IPS)}(J)$, i.e., $C(J)$ evaluated for the TWB and the IPS state, respectively. The behavior is similar to that of $B(J)$, the maximum violation being now $C_{r,\phi,\eta}^{(\rm IPS)}(J)=2.40$ for $\tau_{\rm eff}=0.999$ and $J=1.6\times 10^{-4}$.

Finally, notice that the maximum violation using IPS states is achieved (for both parametrizations) when $\tau_{\rm eff}$ approaches unity and for values of r smaller than for the TWB.

V. NONLOCALITY AND HOMODYNE DETECTION

The Wigner function $W_{r,\phi,\eta}(\alpha,\beta)$ given in Eq. (41) is not positive definite and thus $\rho_{\rm IPS}$ can be used to test the violation of Bell's inequalities by means of homodyne detection, i.e., measuring the quadratures x_ϑ and x_φ of the two IPS modes a and b, respectively, as proposed in Refs. [3] and [4]. In this case, if one discretizes the measured quadratures assuming as outcome +1 when $x\geqslant 0$ and −1 otherwise, one obtains the following Bell parameter:

$$S=E(\vartheta_1,\varphi_1)+E(\vartheta_1,\varphi_2)+E(\vartheta_2,\varphi_1)-E(\vartheta_2,\varphi_2), \quad (43)$$

where ϑ_j and φ_j are the phases of the two homodyne measurements at the modes a and b, respectively, and

$$E(\vartheta_j,\varphi_k)=\int_{\mathbb{R}^2} dx_{\vartheta_j}dx_{\varphi_k}\,\mathrm{sgn}[x_{\vartheta_j}x_{\varphi_k}]P(x_{\vartheta_j},x_{\varphi_k}), \quad (44)$$

$P(x_{\vartheta_j},x_{\varphi_k})$ being the joint probability of obtaining the two outcomes x_{ϑ_j} and x_{φ_k} [4]. As usual, violation of Bell's inequality is achieved when $|S|>2$.

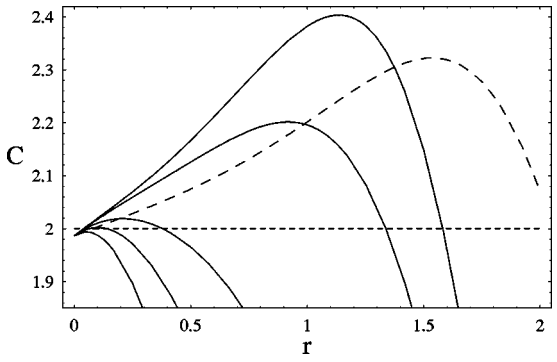

FIG. 4. Plots of $C(J)$ given in Eq. (7) as a function of the squeezing parameter r for $J=1.6\times 10^{-4}$. In all the plots the dashed line is $C_r^{(\rm TWB)}(J)$, while the solid lines are $C_{r,\phi,\eta}^{(\rm IPS)}(J)$ for different values of $\tau_{\rm eff}$ (see the text): from top to bottom $\tau_{\rm eff}=0.999$, 0.99, 0.95, 0.9, and 0.8. When $\tau_{\rm eff}=0.999$ the maximum of $C_{r,\phi,\eta}^{(\rm IPS)}(J)$ is 2.40.

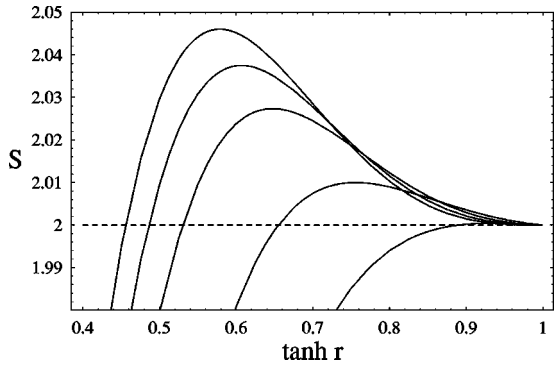

FIG. 5. Plots of S given in Eq. (43) as a function of $\tanh(r)$ for different values of $\tau_{\rm eff}$ and for ideal homodyne detection (i.e., with quantum efficiency $\eta_{\rm H}=1$): from top to bottom $\tau_{\rm eff}=0.99$, 0.95, 0.90, 0.80, and 0.70.

In Fig. 5 we plot S for $\vartheta_1=0$, $\vartheta_2=\pi/2$, $\varphi_1=-\pi/4$, and $\varphi_2=\pi/4$: as pointed out in Ref. [4], Bell's inequality is violated for a suitable choice of the squeezing parameter r. Moreover, when $\tau_{\rm eff}$ decreases the maximum of violation shifts toward higher values of r.

As one expects, taking into account the efficiency $\eta_{\rm H}$ of the homodyne detection further reduces the violation (see Fig. 6). Notice that, when $\eta_{\rm H}<1$, violation occurs for higher values of r, although its maximum is actually reduced: in order to have a significant violation one needs a homodyne efficiency greater than 80% (when $\tau_{\rm eff}=0.99$).

On the other hand, the high efficiencies of this kind of detector allow a loophole-free test of hidden variable theories [13,14], although the violations obtained are quite small. This is due to the intrinsic information loss of the binning process, which is used to convert the continuous homodyne data in dichotomic results [15]. Better results, even if the violation is always small, can be achieved using a *circle* coherent state [13,14] or a superposition of photon number states [15], while maximal violation, i.e., $S=2\sqrt{2}$, is obtained by means of a different binning process, called root binning, and choosing a particular family of quantum states [16,17].

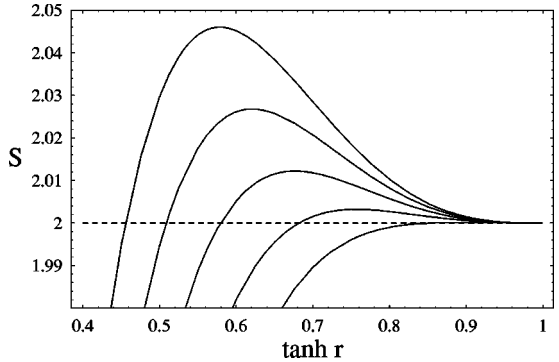

FIG. 6. Plots of S given in Eq. (43) as a function of $\tanh(r)$ with $\tau_{\rm eff}=0.99$ and for different values of the homodyne detection efficiency $\eta_{\rm H}$: from top to bottom $\eta_{\rm H}=1$, 0.95, 0.90, 0.85, and 0.80. The maximum of the violation decreases and shifts toward higher values of r as $\eta_{\rm H}$ decreases. For smaller values of $\tau_{\rm eff}$ the violation is further reduced.

VI. CONCLUDING REMARKS

In this paper we have shown that IPS can be used to produce non-Gaussian two-mode states starting from a TWB. We have studied the nonlocality of IPS states in phase space using the Wigner function. As for the improvement of IPS-assisted teleportation [5], we have found that the nonlocal correlations are enhanced for small energies of the TWB (small squeezing parameter r). Moreover, the nonlocality of ϱ_{IPS} is larger than that of TWB irrespective of the IPS quantum efficiency.

Since the Wigner function of the IPS state is not positive definite, we have also analyzed its nonlocality using homodyne detection. In this case violation of Bell's inequality is much less than in the phase space, and is further reduced for nonunit homodyne efficiency $\eta_{\mathrm{H}}<1$. However, this setup (IPS with homodyning) is of particular interest, since it can be realized with current technology, achieving a loophole-free test of Bell's inequality [3,4].

On the other hand, the experimental verification of phase-space nonlocality is challenging, due to the difficulties of measuring the parity, either directly or through measurement of the photon distribution. However, the recent experimental generation of IPS states [6] is indeed a step toward its implementation.

ACKNOWLEDGMENTS

S.O. would like to express his gratitude to A. R. Rossi and A. Ferraro for stimulating discussions and for their continuous assistance.

[1] U. Leonhardt and J. A. Vaccaro, J. Mod. Opt. **42**, 939 (1995).
[2] K. Banaszek and K. Wódkiewicz, Phys. Rev. A **58**, 4345 (1998).
[3] H. Nha and H. J. Carmichael, Phys. Rev. Lett. **93**, 020401 (2004).
[4] R. García-Patrón Sánchez *et al.*, e-print quant-ph/0403191.
[5] S. Olivares, M. G. A. Paris, and R. Bonifacio, Phys. Rev. A **67**, 032314 (2003).
[6] J. Wenger, R. Tualle-Brouri, and P. Grangier, Phys. Rev. Lett. **92**, 153601 (2004).
[7] J. F. Clauser, M. A. Horne, A. Shimony, and R. A. Holt, Phys. Rev. Lett. **23**, 880 (1969).
[8] A. Ferraro (private communication).
[9] H. Jeong *et al.*, Phys. Rev. A **67**, 012106 (2003).
[10] T. Opatrný, G. Kurizki, and D.-G. Welsch, Phys. Rev. A **61**, 032302 (2000).
[11] P. T. Cochrane, T. C. Ralph, and G. J. Milburn, Phys. Rev. A **65**, 062306 (2002).
[12] M. G. A. Paris, M. Cola, and R. Bonifacio, Phys. Rev. A **67**, 042104 (2003).
[13] A. Gilchrist, P. Deuar, and M. D. Reid, Phys. Rev. Lett. **80**, 3169 (1998).
[14] A. Gilchrist, P. Deuar, and M. D. Reid, Phys. Rev. A **60**, 4259 (1999).
[15] W. J. Munro, Phys. Rev. A **59**, 4197 (1999).
[16] G. Auberson *et al.*, Phys. Lett. A **300**, 327 (2002).
[17] J. Wenger *et al.*, Phys. Rev. A **67**, 012105 (2003).